

Comparative Analysis of HAND with TWI Flood-Prone Mapping Models in Data-Scarce Areas

*Ajun Purwanto¹, Eviliyanto², Donny Andrasgoro³

^{1,2,3} Departement of Geography Education, PGRI Pontianak University, Pontianak, Indonesia

Received: 2024-08-15

Revised: 2024-09-12

Accepted: 2025-03-22

Published: 2025-05-26

Keywords: Evaluation; HAND Model; Flood-Prone; Topographic Wetness Index; Data-scarce areas

Correspondent email:

ajunpurwanto@ikippgriptk.ac.id

Abstract. Flood is one of the most frequent natural disasters in Indonesia and worldwide. Therefore, this study aimed to compare and evaluate flood-prone mapping model using Height Above Nearest Drainage (HAND) and Topographic Wetness Index (TWI) model in data-scarce areas. HAND and TWI models were used to estimate flood-prone level, with field survey and image interpretation as primary methodologies. The data used was Digital Elevation Model (DEM) imagery with a resolution of 10 meters, incorporating elevation, slope, and hydrological parameters namely flow accumulation, direction, and distance. The mapping flood-prone areas were categorized as very prone, prone, moderate, not prone, and very not prone. The results showed that there were differences between HAND and TWI models in terms of area and percentage. The differences in flood inundation characteristics produced by HAND model were mainly due to variations in elevation and proximity to drainage channels. In contrast, TWI model focused on topography, soil moisture, and runoff potential. The differences between the two models also emphasized the importance of terrain characteristics in model predictions. The comparable predictive ability of HAND and TWI models presents an alternative and complementary method for mapping flood-prone locations in data-scarce areas.

©2025 by the authors and Indonesian Journal of Geography

This article is an open access article distributed under the terms and conditions of the Creative Commons Attribution (CC BY NC) license <https://creativecommons.org/licenses/by-nc/4.0/>.

1. Introduction

Flood is one of the most frequent natural disasters in Indonesia and worldwide. This phenomenon impacts millions of people globally and significantly harms both natural and human resources (Henstra et al., 2019; Purwanto et al., 2022, 2024). In this regard, property and infrastructure damage can put human and animal life in jeopardy (Latue et al., 2023; Latue & Rakuasa, 2023). Flood is considered a serious natural disaster (Zeleňáková et al., 2019) and deserves serious attention. It occurs when water overwhelms typically dryland, roads, rivers, and lowlands due to an excess of volume beyond the area drainage or storage capacity (Souissi et al., 2020).

According to data, an estimated 163 floods have been recorded worldwide every year between 2001 and 2020, resulting in \$34.1 billion worth of economic damages (CRED, 2022). About 223 more cases of flood were recorded in 2021, which resulted in significant financial losses of US\$74.4 billion. Factors including conditions of land usage and cover, as well as community development contribute to the continuous trend of flood (Grahn & Nyberg, 2017). Flood danger is projected to rise due to climate change and altered land use and cover, particularly urbanization in floodplains (Thalakkottukara et al., 2024). A warmer climate is expected to increase the danger of flood because of changes in the distribution and variability of precipitation, which affects the hydrological cycle intensity, frequency, and length (Madakumbura et al., 2019). It also affects socioeconomic development variables (Arnell & Gosling, 2016; Madakumbura et al., 2019; Tellman et al., 2021; Winsemius et al., 2016).

In general, spatial heterogeneity is a common characteristic of flood-prone locations (Saharia et al., 2017; Thalakkottukara et al., 2024), with large differences in flood risk between urban and rural areas. At the moment, the majority of study interest is focused on cases from metropolitan regions to rural areas, which are presumably the most sensitive to the effects of floods (Bukvic & Harrald, 2019; Cutter et al., 2016; Rhubarb & Sun, 2021; Thalakkottukara et al., 2024). Lack of access to sufficient data and instruments for studying and assessing flood risk contributes to the rise of distinct regional physical features and the deterioration in flood resistance in rural regions. However, by charting flood regions ahead of time, rural areas degree of flood resilience may be greatly increased since these maps help stakeholders communicate risks (Henstra et al., 2019; Purwanto et al., 2022). Charting flood-prone regions helps lessen the effects of flood and promote the growth of rural communities (Purwanto et al., 2024) that are risk-aware and climate-resilient.

Several hydraulic and hydrodynamic models, including MIKE FLOOD, SMS-SRH, and HEC-RAS, are used for flood mapping (Deslauriers & Mahdi, 2018; Patel et al., 2017). More precise spatial and temporal data are unavailable in rural areas due to numerous constraints (Albano et al., 2020; Coccia et al., 2023; Shastry & Durand, 2019). Therefore, rural communities and emergency managers lack access to flood inundation mapping, which would have helped lessen the effects of flood (Thalakkottukara et al., 2024).

Many models and tools with varying data and computational needs have been created due to various initiatives

focused on mapping floods in areas lacking comprehensive data and observations. For example, Height Above Nearest Drainage (HAND) models have been developed to produce flood inundation maps for flood events from Digital Elevation Model (DEM) (Hu & Demir, 2021a; Nobre et al., 2011; Rennó et al., 2008). The 2D hydrodynamic models can also simulate fluvial at 30 m resolution but only in catchments larger than 50 km² in area (Wing et al., 2017). Additionally, Topographic Wetness Index (TWI) models can serve as an alternative to the conventional method of defining flood-prone areas solely through contouring (Latue & Rakuasa, 2023; Pourali et al., 2016).

HAND is a terrain property generated from DEM that suggests the possibility of drying and soil moisture development. It is a useful descriptor to identify hydrologically unique landscape units (Gharari et al., 2011; Nobre et al., 2011). HAND-based method has several advantages over hydraulic/hydrodynamic models, including decreased complexity and computational efficiency with streamlined input data needs.

The use of hydraulic and hydrodynamic models is limited by excessive data and computational requirements (Thalakkottukara et al., 2024). The main advantages of HAND-based method over hydraulic/hydrodynamic models are computational efficiency and lower complexity with simple input data requirements. Many studies have demonstrated the suitability of HAND models in flood inundation and floodplain mapping studies under various hydro-environmental conditions (Bhatt & Srinivasa Rao, 2018; Diehl et al., 2021; Rahmati et al., 2018; Scriven et al., 2021; Speckhann et al., 2018). HAND is also applied in various web-based flood inundation mapping and real-time flood guidance and forecasting systems (Chaudhuri et al., 2021; Hu & Demir, 2021b; Johnson et al., 2019; Unnithan et al., 2024; Zheng et al., 2018).

Similar to HAND, TWI model offers a cheaper method of flood assessment than using traditional hydrodynamic models. TWI is a method of measuring the level of wetness or soil surface moisture in an area based on topographic characteristics (Nucifera & Putro, 2017). It is based on calculating a topographic index that includes the elevation and slope of an area (Berhanu & Bisrat, 2018; Muin et al., 2023). TWI can be used in various applications, including mapping potential flood areas (Muin et al., 2023), flood-prone areas (watersheds), and flood modeling in watersheds (Rakuasa et al., 2023). Statistical measures that estimate the level of consistency in topography-based methods show that HAND and TWI produce more plausible floodplain maps (Dhote et al., 2023).

In general, data-scarce areas will hinder the process of mapping flood vulnerability. The condition of the regions in West Kalimantan is mostly data-scarce provision, but HAND and TWI models allow flood mapping to be carried out despite data scarcity. Therefore, this study aimed to compare and analyze the flood-prone mapping model using HAND and TWI models in Serawai Sub-watershed. The results are expected to offer answers for the problems of flood mapping in West Kalimantan and other data-scarce areas.

2. Methods

Study Area

Astronomically, the study area is located between 112°25'00" E - 112°46'30" E and latitude 0°30'00" S - 0°45'00" S (Figure 1) with a total area of approximately 171.542,39 ha.

The location is bounded to the east, north, and west by Kapuas sub-watershed, and to the south by Ketingan sub-watershed.

Method

The method used in this study was survey and image interpretation. The data collected include topographic maps and DEM images with a resolution of 10 meters from ALOS Palsar.

a. Basic Digital Elevation Model processing

Basic digital altitude model processing of the area was carried out to obtain a basic information layer for estimating flood area. The flow direction was established after any depressions had been eliminated. Each pixel flow direction was given to one of the eight neighbors (D8 - Deterministic Eight-Neighbor method) (Dantas & Paz, 2021; Jenson & Domingue, 1988; Mark, 1984).

The primary criterion for determining flow direction is to orient it toward the neighboring pixel with the steepest slope. However, there are also particular guidelines for treating depressions and planes depending on the algorithm, which typically requires changing the height (Barnes et al., 2014). In general, the flow direction determines the accumulated drainage area. This area comprises a raster layer with each pixel attribute representing an upstream contribution area, the total of all the pixel areas whose flow routes lead to that pixel.

b. Drainage Network Determination

The drainage network was established based on the cumulative drainage area, calculated by applying a threshold to the accumulated area (Fan et al., 2013; Goerl et al., 2017; Momo et al., 2016; Speckhann et al., 2018). In other words, network drainage was represented by all watershed pixels, with drainage areas more significant than the threshold. Different threshold values that reflect the drainage network's sensitivity are more than or equal to 100.

c. Combining Existing Vector Drainage Networks

DEM processing method, known as stream flaring, has been used to define the flow route in a manner compatible with the vector network representation of DEM river drainage network (Lindsay, 2016; Wu et al., 2019). With the exact DEM spatial resolution, the vector network transformed to a raster format, and DEM pixels directly adjacent to the vector network representative pixels were reduced in height. Similar to DEM without river burning, this modified DEM was processed to derive flow directions, accumulation areas, basin borders, and drainage networks while removing basins.

ArcGIS Pro, which includes a DEM processing system, was used to determine HAND terrain descriptors in the form of flow directions, basin borders, and drainage networks formatted as raster. The height (Z_p) of each basin pixel which was not a component of the drainage network, was identified. The downstream flow path was then monitored, until it reached the drainage network, recording the elevation (Z_r) of the corresponding drainage network pixel. Furthermore, the topography reference of HAND changes (Dantas & Paz, 2021; Nobre et al., 2011), and a corresponding referential (Z_r) were assigned to each pixel. HAND was determined based on the difference between Z_p and Z_r . Subsequently, the flood area was estimated in a standard way by reclassifying HAND value with

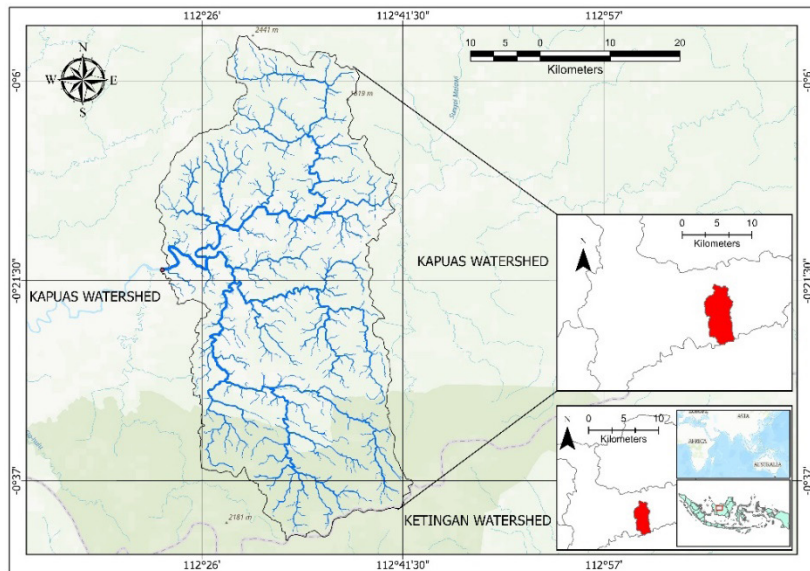


Figure 1. Study Area

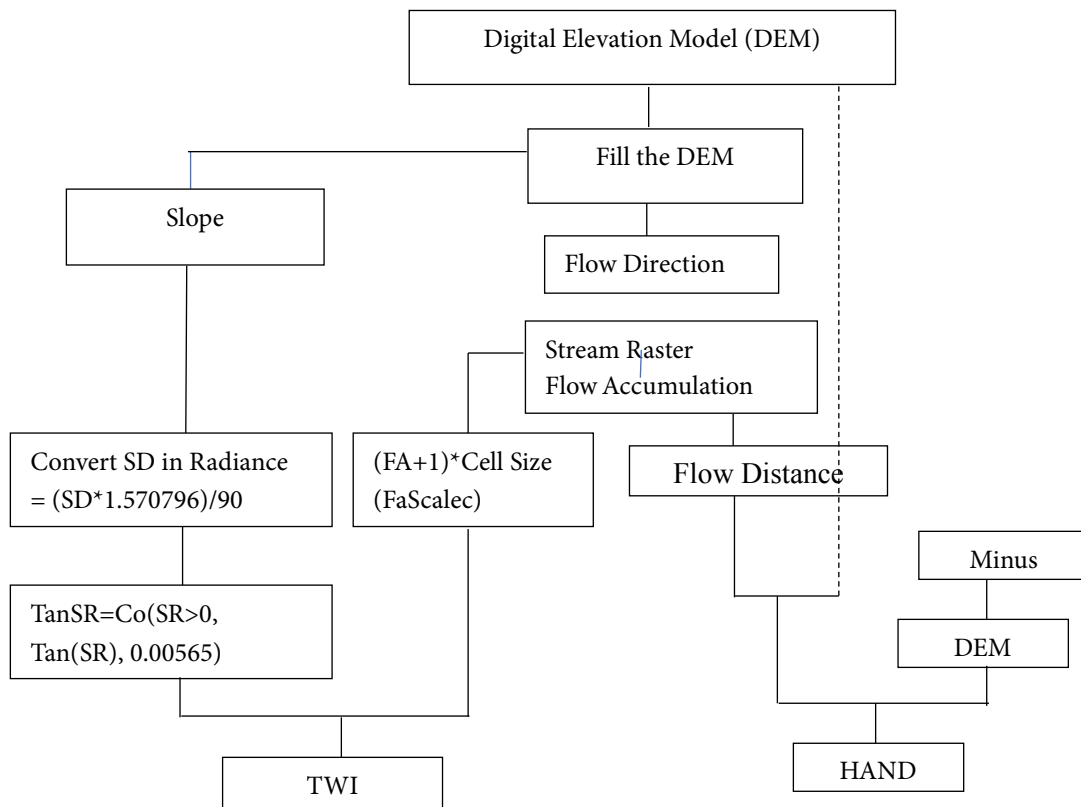


Figure 2. Study Method

scoring from very prone, prone, moderate, non-prone, and very non-prone. The stages of the methodology are shown in Figure 2.

Data Analysis

ArcGIS Pro was used for data analysis, specifically Hydrology Spatial Analysis tool including filling, flow accumulation, flow direction, and flow distance. HAND value was obtained using Mathematical analysis through the Minus tool in ArcGIS Pro. Additionally, TWI value was obtained using the Map Algebra and Reclassification tools to determine the level of flood vulnerability in the study area.

3. Result and Discussion

The main factor influencing flood is altitude, with flood risk increasing as elevation decreases (Choubin et al., 2019; Mumbai, 2020). During the rainy season, low-lying areas are flooded almost every year. The elevation information in this study was obtained from DEM data, which was classified using ArcGIS Pro into five classes (Althuwaynee et al., 2012; Bui et al., 2019). Elevation maps were created and classified using the reclassify tool in ArcGIS Pro. The five elevation class areas include 0 - 45 m, 45 - 107 m, 107 - 160 m, 160 - 206 m, and 206 - 254 m. The altitude classification of the study area is shown in Figure 3.

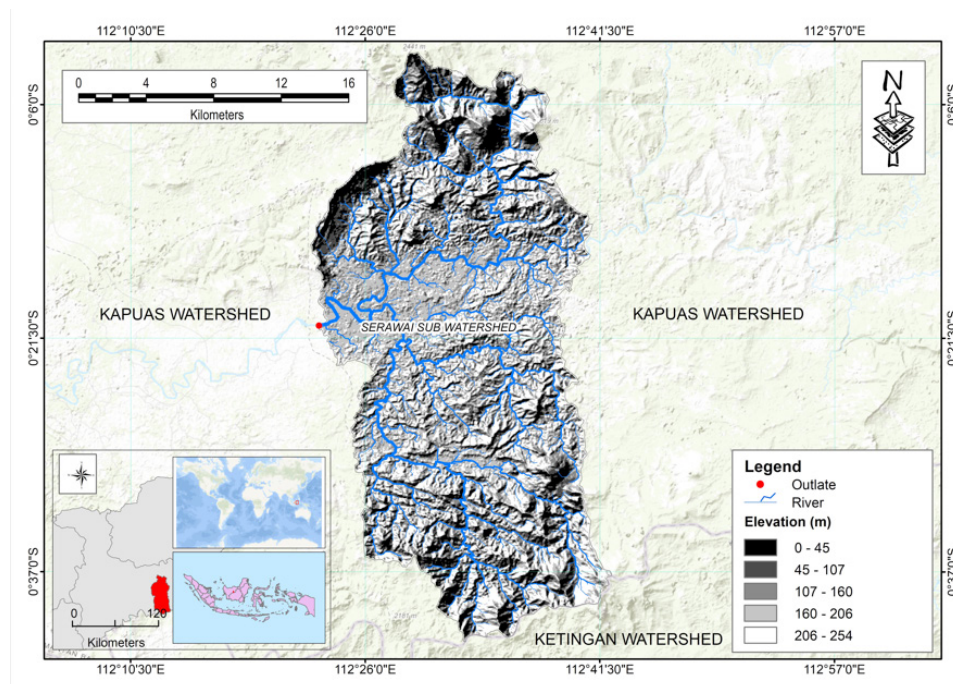


Figure 3. Watershed Altitude

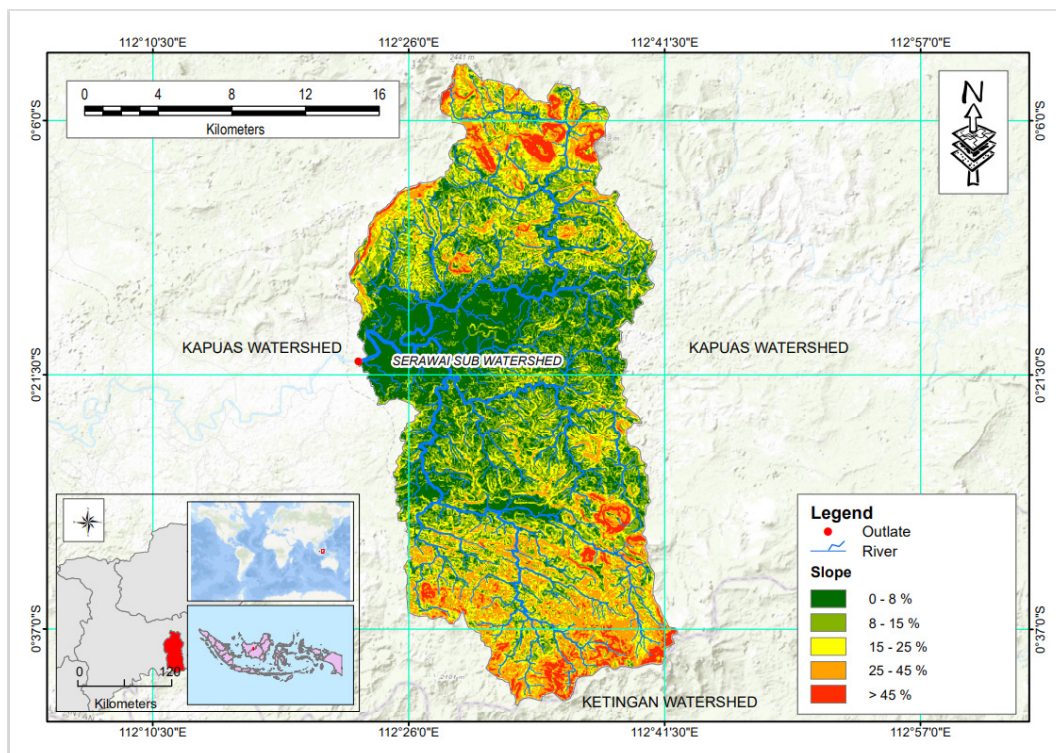


Figure 4. Watershed Slope

Aside from elevation, slope has a significant influence on flood-prone areas (Alemayehu, 2007; Wondim, 2016). The rate at which surface water moves through drainage channels and watersheds is significantly influenced by slope (Hu & Demir, 2021b). Consequently, slope has the effect of increasing surface water runoff and peak discharge with higher slope steepness. Slope of 0-8% occupy most of the subwatershed, suggesting that most of the subwatershed is very vulnerable to flood hazards. Flat land is more susceptible to flood, while water easily flows as surface runoff in steep areas. Compared to steeper locations, flat places are more likely to flood because water travels more slowly there and accumulates over time

(Desalegn & Mulu, 2021; Gigović et al., 2017; Hagos et al., 2022; Rimba et al., 2017; Singh et al., 2020; Wondim, 2016). Slope of the study area is presented in Figure 4.

The geomorphological element associated with flood is distance from the river. In general, distance from the river is used because flow affects slope stability. River flow cuts the toe of slope or partially submerges the material below the water table (Mojaddadi et al., 2017). Distance is reflected by the proximity of the river or drainage, represented by the river flow pattern. River distance maps were created using the Euclidean tool with ArcGIS Pro.

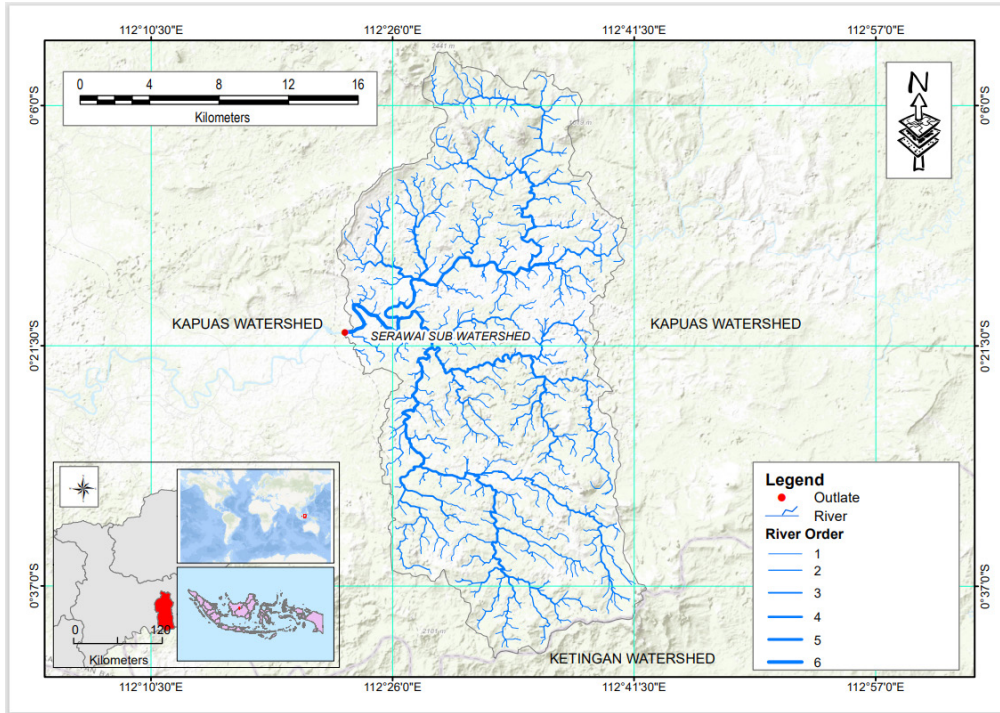


Figure 5. Flow Pattern

Table 1. Area of Flood-Prone with HAND

Prone Classes	Area (Ha)	%
Very prone	111.902,37	65,35
Prone	29.356,65	17,14
Moderate	18.971,52	11,08
Not prone	7.996,20	4,67
Very not prone	3.004,20	1,75
	17.1230,94	100,00

Source: secondary data processing (2024)

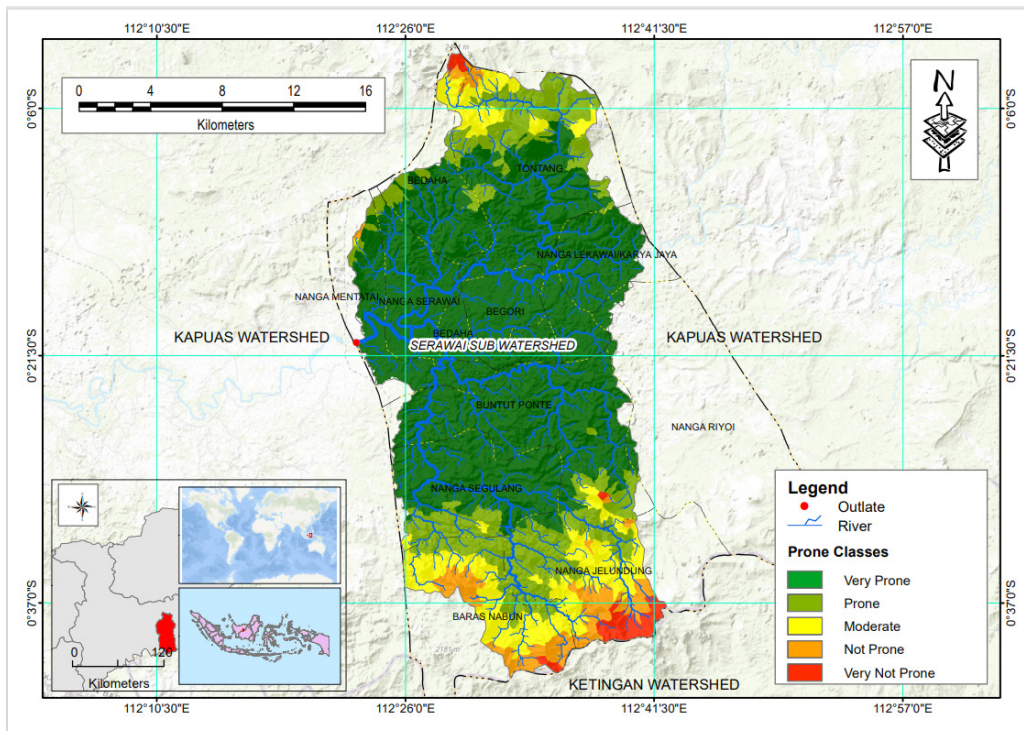


Figure 5. Area and Distribution of Flood-Prone with HAND

The distance from the river has a substantial impact on the distribution and severity of floods in a given region (Bui et al., 2019; Grayson & Ladson, 1991). High-intensity rainfall events create significant water runoff around nearby rivers in areas with insufficient infiltration and percolation because of changes in soil properties, vegetation cover, and land surface slope (Bui et al., 2019; Kia et al., 2012). This can lead to catastrophic flood in downstream areas with lower topographic gradients.

HAND was created by using DEM data, through Geographic Information System (GIS) software, ArcGIS Pro. Data were collected on flow direction and flow distance that have been processed using the Minus tool in spatial analysis. The results showed that Serawai sub-watershed has five classes of vulnerability, namely very prone, prone, moderate, not prone, and very not prone. HAND analysis results for the distribution and extent of flood-prone are shown in Table 1.

Very prone class has an area of 111,902.37 ha (65.35%), including the villages of Tontang, Sedaha, Nanga Serawai, Begori, Nanga Lekawai, Surgaa, Buntut Ponte, and Nanga Segulang. Areas with a high level of prone amounted to 29,356.65 ha (17.14%). Meanwhile, areas with a high level of prone are spread across the villages of Beurgea, Nanga Segulang, Nanga Jelundung, and Tontang. Moderate-prone

areas amounted to 18,971.52 ha (11.08%), spreading across the villages of Tontang, Nanga Jelundung, and Baras Nabun. The areas with not prone level were 7,996.20 ha (4.67%), spread across parts of Baras Nabun and parts of Nanga Jelundung. Finally, very not prone areas were estimated at 3,004.20 (1.75%), spreading across villages of Sedaha, Baras Nabun, and Nanga Jelundung.

Based on the calculation and mapping results of TWI in the study area, the lowest and highest values were 4.148 and 23.593, respectively. The range was then classified into five classes with the quantile method.

The results of TWI analysis for the distribution and extent of flooding are shown in Table 2:

HAND measures the relative elevation of each point in the landscape above the nearest drainage channel (Dhote et al., 2023). The model is particularly useful for identifying areas prone to flood by determining the water level required to inundate a given location. HAND is effective in delineating floodplains and assessing flood risk based on proximity and elevation relative to water bodies. On the other hand, TWI combines slope and upstream contributing areas to estimate potential soil moisture (Berhanu & Bisrat, 2018; Dhote et al., 2023; Muin et al., 2023; Purwanto, 2023). It is a measure of how likely an area is to retain water, indicating areas prone

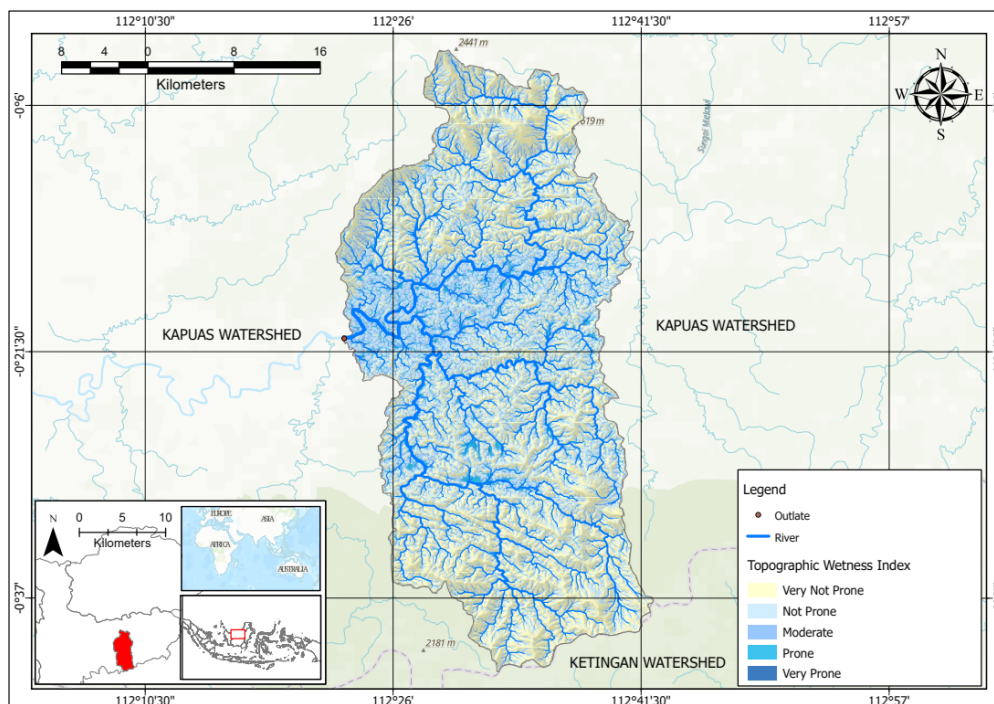


Figure 5. Area and Distribution of Flood-Prone with HAND

Table 2. Area of Flood-Prone with TWI

Prone Classes	Area (Ha)	%
Very prone	75.821,241	44,29
Prone	57462,786	33,56
Moderate	22125,526	12,92
Not prone	12152,991	7,10
Very not prone	3668,396	2,14
	17.1230,94	100,00

Source: secondary data processing (2024)

to saturation and runoff. TWI is often used to predict soil moisture patterns, runoff generation, and erosion, rather than direct flood risk (Kok & Kim, 2019; Raduła et al., 2018; Winzeler et al., 2022).

According to different studies, HAND model directly focuses on identifying flood-prone areas based on elevation and proximity to water bodies (Hu & Demir, 2021b; Komolafe et al., 2020; Purwanto, 2023; Sabeh et al., 2025). The model is particularly useful for floodplain management and emergency response planning. Inundation mapping can be used to simulate various flood scenarios by adjusting the water level in the drainage network (Hu & Demir, 2021b). On the other hand, TWI model is more focused on understanding hydrological processes such as runoff, soil moisture distribution, and erosion risk. It is effective for identifying areas likely to be saturated, which contribute to floods, landslides, and other hydrological hazards (Li & Demir, 2022; Mhiret et al., 2019).

HAND model provides a direct interpretation of flood risk based on water surface elevation. Areas with low HAND values have a higher flood risk. Flood-prone areas can be assessed by setting certain elevation limits above the drainage network. Meanwhile, TWI model shows that wet or saturated areas are not directly correlated with flood distribution. High TWI values imply potential areas of water accumulation, indicating high surface runoff during heavy rainfall events (Berhanu & Bisrat, 2018; Qiu et al., 2020).

4. Conclusion

In conclusion, this study showed differences in the results of flood hazard mapping using HAND and TWI models. The differences in flood vulnerability results between both models can be attributed to variations in methodologies and applications. HAND model is directly related to elevation and proximity to drainage channels, making it more suitable for direct mapping of floodplains and water bodies. In contrast, TWI model focuses on topographic wetness and hydrological processes, providing insight into soil moisture and potential runoff, which can indirectly inform flood risk. Both models provide an alternative, flood-prone area mapping in data-scarce areas.

Acknowledgment

The authors are grateful to Kemenristekdikti for the financial support for grants.

References

- Albano, R., Samela, C., Crăciun, I., Manfreda, S., & ... (2020). Large scale flood risk mapping in data scarce environments: An application for Romania. *Water*. <https://doi.org/10.3390/w12061834>.
- Alemayehu, Z. (2007). *Modeling of Flood hazard management for forecasting and emergency response of 'Koka' area within Awash River basin using remote sensing and GIS method*. Addis Ababa University.
- Althwaynee, O. F., Pradhan, B., & Lee, S. (2012). Computers & Geosciences Application of an evidential belief function model in landslide susceptibility mapping. *Computers and Geosciences*, 44, 120–135. <https://doi.org/10.1016/j.cageo.2012.03.003>.
- Arnell, N. W., & Gosling, S. N. (2016). The impacts of climate change on river flood risk at the global scale. *Climatic Change*, 134, 387–401. <https://doi.org/10.1007/s10584-014-1084-5>.
- Barnes, R., Lehman, C., & Mulla, D. (2014). An efficient assignment of drainage direction over flat surfaces in raster digital elevation models. *Computers & Geosciences*, 62, 128–135. <https://doi.org/10.1016/j.cageo.2013.01.009>.
- Berhanu, B., & Bisrat, E. (2018). Identification of surface water storing sites using topographic wetness index (TWI) and normalized difference vegetation index (NDVI). *JNRD-Journal of Natural Resources and Development*, 8, 91–100. <https://doi.org/10.1007/s12517-018-3952-1>.
- Bhatt, C. M., & Srinivasa Rao, G. (2018). HAND (height above nearest drainage) tool and satellite-based geospatial analysis of Hyderabad (India) urban floods, September 2016. *Arabian Journal of Geosciences*, 11(19), 600. <https://doi.org/10.1007/s12517-018-3952-1>.
- Bui, D. T., Khosravi, K., Shahabi, H., & Daggupati, P. (2019). *Flood Spatial Modeling in Northern Iran Using Remote Sensing and GIS: A Comparison between Evidential Belief Functions and Its Ensemble with a Multivariate Logistic Regression Model*. <https://doi.org/10.3390/rs11131589>.
- Bukvic, A., & Harrald, J. (2019). Rural versus urban perspective on coastal flood: The insights from the US Mid-Atlantic communities. *Climate Risk Management*, 23, 7–18. <https://doi.org/10.1016/j.crm.2018.10.004>.
- Chaudhuri, C., Gray, A., & Robertson, C. (2021). InundatEd-v1.0: a height above nearest drainage (HAND)-based flood risk modeling system using a discrete global grid system. *Geoscientific Model Development*, 14(6), 3295–3315. <https://doi.org/10.5194/gmd-14-3295-2021>.
- Choubin, B., Moradi, E., Golshan, M., Adamowski, J., Sajedi-Hosseini, F., & Mosavi, A. (2019). An ensemble prediction of flood susceptibility using multivariate discriminant analysis, classification and regression trees, and support vector machines. *Science of the Total Environment*, 651, 2087–2096. <https://doi.org/10.1016/j.scitotenv.2018.10.064>.
- Coccia, G., Ceresa, P., Bussi, G., Denaro, S., Bazzurro, P., Martina, M., Fagà, E., Avelar, C., Ordaz, M., & Huerta, B. (2023). Large-scale flood risk assessment in data scarce areas: an application to Central Asia. *Natural Hazards and Earth System Sciences Discussions*, 2023, 1–33. <https://doi.org/10.5194/nhess-2023-157>.
- Cutter, S. L., Ash, K. D., & Emrich, C. T. (2016). Urban–rural differences in disaster resilience. *Annals of the American Association of Geographers*, 106(6), 1236–1252. <https://doi.org/10.1080/24694452.2016.1194740>.
- Dantas, A. A. R., & Paz, A. R. (2021). Use of HAND terrain descriptor for estimating flood-prone areas in river basins. *Brazilian Journal of Environmental Sciences (Online)*, 56(3), 501–516. <https://doi.org/10.5327/Z21769478892>.
- Desalegn, H., & Mulu, A. (2021). Flood vulnerability assessment using GIS at Fetam watershed, upper Abbay basin, Ethiopia. *Heliyon*, 7(1), e05865. <https://doi.org/10.1016/j.heliyon.2020.e05865>.
- Deslauriers, S., & Mahdi, T.-F. (2018). Flood modelling improvement using automatic calibration of two dimensional river software SRH-2D. *Natural Hazards*, 91, 697–715. <https://doi.org/10.1007/s11069-017-3150-6>.
- Dhote, P. R., Joshi, Y., Rajib, A., Thakur, P. K., Nikam, B. R., & Aggarwal, S. P. (2023). Evaluating topography-based approaches for fast floodplain mapping in data-scarce complex-terrain regions: Findings from a Himalayan basin. *Journal of Hydrology*, 620, 129309. DOI [10.1016/j.jhydrol.2023.129309](https://doi.org/10.1016/j.jhydrol.2023.129309).
- Diehl, R. M., Gourevitch, J. D., Drago, S., & Wemple, B. C. (2021). Improving flood hazard datasets using a low-complexity, probabilistic floodplain mapping approach. In *PloS one*. journals.plos.org. <https://journals.plos.org/plosone/article?id=10.1371/journal.pone.0248683>. <https://doi.org/10.1371/journal.pone.0248683>.
- Fan, F. M., Collischonn, W., Sorribas, M. V., & Pontes, P. R. M. (2013). Sobre o início da rede de drenagem definida a partir

- dos modelos digitais de elevação. *Rbrh: Revista Brasileira de Recursos Hídricos. Porto Alegre, RS. Vol. 18, n. 3 (Jul./Set. 2013), p. 241-257.* <https://doi.org/10.21168/rbrh.v18n3.p241-257>
- Gharari, S., Hrachowitz, M., Fenicia, F., & Savenije, H. H. G. (2011). Hydrological landscape classification: investigating the performance of HAND based landscape classifications in a central European meso-scale catchment. *Hydrology and Earth System Sciences, 15*(11), 3275–3291. <https://doi.org/10.5194/hess-15-3275-2011>.
- Gigović, L., Pamučar, D., Bajić, Z., & Drobnjak, S. (2017). Application of GIS-interval rough AHP methodology for flood hazard mapping in urban areas. *Water, 9*(6), 360. <https://doi.org/10.3390/w9060360>.
- Goerl, R. F., Michel, G. P., & Kobiyama, M. (2017). Mapeamento de áreas suscetíveis a inundação com o modelo HAND e análise do seu desempenho em diferentes resoluções espaciais. *Revista Brasileira de Cartografia, 69*(1). <https://doi.org/10.14393/rbcv69n1-44032>.
- Grahn, T., & Nyberg, L. (2017). Assessment of pluvial flood exposure and vulnerability of residential areas. *International Journal of Disaster Risk Reduction, 21*, 367–375. <https://doi.org/10.1016/j.ijdrr.2017.01.016>.
- Grayson, R. B., & Ladson, A. R. (1991). DIGITAL TERRAIN MODELLING: A REVIEW OF HYDROLOGICAL, GEOMORPHOLOGICAL, AND BIOLOGICAL APPLICATIONS. 5(September 1990), 3–30. <https://doi.org/10.1002/hyp.3360050103>.
- Hagos, Y. G., Andualem, T. G., Yibeltal, M., & Mengie, M. A. (2022). Flood hazard assessment and mapping using GIS integrated with multi-criteria decision analysis in upper Awash River basin, Ethiopia. *Applied Water Science, 12*(7), 1–18. <https://doi.org/10.1007/s13201-022-01674-8>.
- Henstra, D., Minano, A., & Thistlethwaite, J. (2019). Communicating disaster risk? An evaluation of the availability and quality of flood maps. *Natural Hazards and Earth System Sciences, 19*(1), 313–323.
- Hu, A., & Demir, I. (2021a). Real-time flood mapping on client-side web systems using hand model. *Hydrology, 8*(2), 65. <https://doi.org/10.3390/hydrology8020065>.
- Hu, A., & Demir, I. (2021b). Real-time flood mapping on client-side web systems using hand model. *Hydrology*. <https://www.mdpi.com/1067816>. <https://doi.org/10.31223/X5M02R>.
- Jenson, S. K., & Domingue, J. O. (1988). Extracting topographic structure from digital elevation data for geographic information system analysis. *Photogrammetric Engineering and Remote Sensing, 54*(11), 1593–1600.
- Johnson, J. M., Munasinghe, D., & ... (2019). An integrated evaluation of the national water model (NWM)–Height above nearest drainage (HAND) flood mapping methodology. In *Natural Hazards and ...* nness.copernicus.org. <https://doi.org/10.5194/nhess-19-2405-2019>.
- Kia, M. B., Pirasteh, S., Pradhan, B., Mahmud, A. R., Nor, W., Sulaiman, A., & Moradi, A. (2012). An artificial neural network model for flood simulation using GIS: Johor River Basin, Malaysia. 251–264. <https://doi.org/10.1007/s12665-011-1504-z>. <https://doi.org/10.1007/s12665-011-1504-z>
- Kok, K., & Kim, J.-C. (2019). Identification of vulnerable regions to soil loss under the dynamic saturation process. *Science of the Total Environment, 659*, 1209–1223. DOI: [10.1016/j.scitotenv.2018.12.398](https://doi.org/10.1016/j.scitotenv.2018.12.398)
- Komolafe, A. A., Awe, B. S., Olorunfemi, I. E., & Oguntunde, P. G. (2020). Modelling flood-prone area and vulnerability using integration of multi-criteria analysis and HAND model in the Ogun River Basin, Nigeria. *Hydrological Sciences Journal, 65*(10), 1766–1783. <https://doi.org/10.1080/02626667.2020.1764960>.
- Latue, P. C., Imanuel Septory, J. S., Somae, G., & Rakuasa, H. (2023). Pemodelan Daerah Rawan Banjir di Kecamatan Sirimau Menggunakan Metode Multi-Criteria Analysis (MCA). *Jurnal Perencanaan Wilayah Dan Kota, 18*(1), 10–17. <https://doi.org/10.29313/jpwk.v18i1.1964>.
- Latue, P. C., & Rakuasa, H. (2023). Identification of Flood-Prone Areas Using the Topographic Wetness Index Method in Fena Leisela District, Buru Regency. *Journal Basic Science and Technology, 12*(1), 20–24. DOI: [10.1016/j.scitotenv.2022.154420](https://doi.org/10.1016/j.scitotenv.2022.154420).
- Li, Z., & Demir, I. (2022). A comprehensive web-based system for flood inundation map generation and comparative analysis based on height above nearest drainage. *Science of The Total Environment, 828*, 154420. DOI: [10.1016/j.scitotenv.2022.154420](https://doi.org/10.1016/j.scitotenv.2022.154420).
- Lindsay, J. B. (2016). The practice of DEM stream burning revisited. *Earth Surface Processes and Landforms, 41*(5), 658–668. <https://doi.org/10.1002/esp.3888>.
- Madakumbura, G. D., Kim, H., Utsumi, N., Shiogama, H., Fischer, E. M., Seland, Ø., Scinocca, J. F., Mitchell, D. M., Hirabayashi, Y., & Oki, T. (2019). Event-to-event intensification of the hydrologic cycle from 1.5 C to a 2 C warmer world. *Scientific Reports, 9*(1), 3483. <https://doi.org/10.1038/s41598-019-39936-2>
- Mark, D. M. (1984). Part 4: mathematical, algorithmic and data structure issues: automated detection of drainage networks from digital elevation models. *Cartographica: The International Journal for Geographic Information and Geovisualization, 21*(2–3), 168–178. <https://doi.org/10.3138/10LM-4435-6310-251R>.
- Mhired, D. A., Dagne, D. C., Assefa, T. T., Tilahun, S. A., Zaitchik, B. F., & Steenhuis, T. S. (2019). Erosion hotspot identification in the sub-humid Ethiopian highlands. *Ecohydrology & Hydrobiology, 19*(1), 146–154. DOI: [10.1016/j.ecohyd.2018.08.004](https://doi.org/10.1016/j.ecohyd.2018.08.004).
- Mojaddadi, H., Pradhan, B., Nampak, H., Ahmad, N., & Halim, A. (2017). Ensemble machine-learning-based geospatial approach for flood risk assessment using multi-sensor remote-sensing data and GIS. 5705(March). <https://doi.org/10.1080/19475705.2017.1294113>.
- Momo, M. R., Pinheiro, A., Severo, D. L., Cuartas, L. A., & Nobre, A. D. (2016). Desempenho do modelo HAND no mapeamento de áreas suscetíveis à inundação usando dados de alta resolução espacial. *RBRH, 21*, 200–208. <https://doi.org/10.21168/rbrh.v21n1.p200-208>.
- Muin, A., Somae, G., & Rakuasa, H. (2023). Analisis Potensi Genangan Banjir di Kecamatan Siwalalat, Kabupaten Seram Bagian Timur berdasarkan Topographic Wetness Index. *ULIL ALBAB: Jurnal Ilmiah Multidisiplin, 2*(5), 1800–1806. DOI: [10.56799/jim.v2i5.1502](https://doi.org/10.56799/jim.v2i5.1502).
- Mumbai, G. (2020). frequency ratio and fuzzy gamma operator models in GIS: a case study of Urban flood susceptibility zonation mapping using evidential belief function, frequency ratio and fuzzy gamma operator models in GIS: a case study of Greater Mumbai, Maharashtra. *Geocarto International, 0*(0), 1–26. <https://doi.org/10.1080/10106049.2020.1730448>.
- Nobre, A. D., Cuartas, L. A., Hodnett, M., Rennó, C. D., Rodrigues, G., Silveira, A., & Saleska, S. (2011). Height Above the Nearest Drainage—a hydrologically relevant new terrain model. *Journal of Hydrology, 404*(1–2), 13–29. <https://doi.org/10.1016/j.jhydrol.2011.03.051>.
- Nucifera, F., & Putro, S. T. (2017). Deteksi Kerawanan Banjir Genangan Menggunakan Topographic Wetness Index (TWI). *Media Komunikasi Geografi, 18*(2), 107–116.
- Patel, D. P., Ramirez, J. A., Srivastava, P. K., Bray, M., & Han, D. (2017). Assessment of flood inundation mapping of Surat city by coupled 1D/2D hydrodynamic modeling: a case application of the new HEC-RAS 5. *Natural Hazards*. <https://doi.org/10.1007/s11069-017-2956-6>.
- Pourali, S. H., Arrowsmith, C., Chrisman, N., Matkan, A. A., & Mitchell, D. (2016). Topography wetness index application in flood-risk-based land use planning. *Applied Spatial Analysis and Policy, 9*, 39–54. <https://doi.org/10.1007/s12061-014-9130-2>.

- Purwanto, A. (2023). Height Above Nearest Drainage (HAND) as a Model for Rapid Flood Inundation Mapping Based on Remote Sensing and Geographic Information Systems in the Kapuas Sintang Sub Watershed. *Jurnal Penelitian Pendidikan IPA*, 9(8), 5899–5905. DOI: [10.29303/jppipa.v9i8.3037](https://doi.org/10.29303/jppipa.v9i8.3037).
- Purwanto, A., Andrasmo, D., & Eviliyanto, E. (2024). Flood Vulnerability Analysis Based on GIS and Remote Sensing at Silat Hulu. *Indonesian Journal of Geography*, 56(2). <https://doi.org/10.22146/ijg.91114>.
- Purwanto, A., Rustam, R., Andrasmo, D., & Eviliyanto, E. (2022). Flood Risk Mapping Using GIS and Multi-Criteria Analysis at Nanga Pinoh West Kalimantan Area. *Indonesian Journal of Geography*, 54(3). <https://doi.org/10.22146/ijg.69879>.
- Qiu, Z., Lyon, S. W., & Creveling, E. (2020). Defining a topographic index threshold to delineate hydrologically sensitive areas for water resources planning and management. *Water Resources Management*, 34(11), 3675–3688. DOI: 10.1007/s11269-020-02643-z.
- Raduła, M. W., Szymura, T. H., & Szymura, M. (2018). Topographic wetness index explains soil moisture better than bioindication with Ellenberg's indicator values. *Ecological Indicators*, 85, 172–179. <https://doi.org/10.1016/j.ecolind.2017.10.011>.
- Rahmati, O., Kornejadi, A., Samadi, M., Nobre, A. D., & Melesse, A. M. (2018). Development of an automated GIS tool for reproducing the HAND terrain model. *Environmental Modelling & Software*, 102, 1–12. <https://doi.org/10.1016/j.envsoft.2018.01.004>.
- Rakuasa, H., Wahab, W. A., Kamiludin, K., Jaelani, A., Ramdhani, R., & Rinaldi, M. (2023). Pemetaan Genangan Banjir di Jalan TB. Simatupang, Jakarta Selatan oleh Unit Pengelola, Penyelidikan, Pengukuran dan Pengujian (UP4) Dinas Sumber Daya Air DKI Jakarta. *Jurnal Altifani Penelitian Dan Pengabdian Kepada Masyarakat*, 3(2), 288–295. <https://doi.org/10.59395/altifani.v3i2.379>.
- Rennó, C. D., Nobre, A. D., Cuartas, L. A., Soares, J. V., Hodnett, M. G., & Tomasella, J. (2008). HAND, a new terrain descriptor using SRTM-DEM: Mapping terra-firme rainforest environments in Amazonia. *Remote Sensing of Environment*, 112(9), 3469–3481. <https://doi.org/10.1016/j.rse.2008.03.018>.
- Rhubart, D., & Sun, Y. (2021). The social correlates of flood risk: variation along the US rural–urban continuum. *Population and Environment*, 43, 232–256. <https://doi.org/10.1007/s11111-021-00388-4>.
- Limba, A. B., Setiawati, M. D., Sambah, A. B., & Miura, F. (2017). Physical flood vulnerability mapping applying geospatial techniques in Okazaki City, Aichi Prefecture, Japan. *Urban Science*, 1(1), 7. <https://doi.org/10.3390/urbansci1010007>.
- Sabeh, H., Abdallah, C., Chahinian, N., Tournoud, M.-G., Hdeib, R., & Moussa, R. (2025). Evaluating terrain-based HAND-SRC flood mapping model in low-relief rural plains using high resolution topography and crowdsourced data. *Journal of Hydrology*, 132649. <https://doi.org/10.1016/j.jhydrol.2024.132649>.
- Saharia, M., Kirstetter, P.-E., Vergara, H., Gourley, J. J., & Hong, Y. (2017). Characterization of floods in the United States. *Journal of Hydrology*, 548, 524–535. <https://doi.org/10.1016/j.jhydrol.2017.03.010>.
- Scriven, B. W. G., McGrath, H., & Stefanakis, E. (2021). GIS derived synthetic rating curves and HAND model to support on-the-fly flood mapping. *Natural Hazards*, 109, 1629–1653. <https://doi.org/10.1007/s11069-021-04892-6>.
- Shastri, A., & Durand, M. (2019). Utilizing flood inundation observations to obtain floodplain topography in data-scarce regions. *Frontiers in Earth Science*, 6, 243. <https://doi.org/10.3389/feart.2018.00243>.
- Singh, A. P., Arya, A. K., & Singh, D. Sen. (2020). Morphometric analysis of Ghaghara River Basin, India, using SRTM data and GIS. *Journal of the Geological Society of India*, 95(2), 169–178. <https://doi.org/10.1007/s12594-020-1406-3>.
- Souissi, D., Zouhri, L., Hammami, S., & ... (2020). GIS-based MCDM–AHP modeling for flood susceptibility mapping of arid areas, southeastern Tunisia. *Geocarto ...* <https://doi.org/10.1080/10106049.2019.1566405>.
- Speckhann, G. A., Chaffe, P. L. B., & ... (2018). Flood hazard mapping in Southern Brazil: a combination of flow frequency analysis and the HAND model. *Hydrological ...* <https://doi.org/10.1080/02626667.2017.1409896>.
- Tellman, B., Sullivan, J. A., Kuhn, C., Kettner, A. J., Doyle, C. S., Brakenridge, G. R., Erickson, T. A., & Slayback, D. A. (2021). Satellite imaging reveals increased proportion of population exposed to floods. *Nature*, 596(7870), 80–86. <https://doi.org/10.1038/s41586-021-03695-w>.
- Thalakkottukara, N. T., Thomas, J., Watkins, M. K., Holland, B. C., Oommen, T., & Grover, H. (2024). Suitability of the height above nearest drainage (HAND) model for flood inundation mapping in data-scarce regions: a comparative analysis with hydrodynamic models. *Earth Science Informatics*, 17(3), 1907–1921. <https://doi.org/10.1007/s12145-023-01218-x>.
- Unnithan, S. L. K., Biswal, B., Rüdiger, C., & Dubey, A. K. (2024). A novel conceptual flood inundation model for large scale data-scarce regions. *Environmental Modelling & Software*, 171, 105863. <https://doi.org/10.1016/j.envsoft.2023.105863>.
- Wing, O. E. J., Bates, P. D., Sampson, C. C., Smith, A. M., Johnson, K. A., & Erickson, T. A. (2017). Validation of a 30 m resolution flood hazard model of the conterminous United States. *Water Resources Research*, 53(9), 7968–7986. <https://doi.org/10.1002/2017WR020917>.
- Winsemius, H. C., Aerts, J. C. J. H., Van Beek, L. P. H., Bierkens, M. F. P., Bouwman, A., Jongman, B., Kwadijk, J. C. J., Ligtoet, W., Lucas, P. L., & Van Vuuren, D. P. (2016). Global drivers of future river flood risk. *Nature Climate Change*, 6(4), 381–385. <https://doi.org/10.1038/nclimate2893>.
- Winzeler, H. E., Owens, P. R., Read, Q. D., Libohova, Z., Ashworth, A., & Sauer, T. (2022). Topographic wetness index as a proxy for soil moisture in a hillslope catena: flow algorithms and map generalization. *Land*, 11(11), 2018. <https://doi.org/10.3390/land11112018>.
- Wondim, Y. K. (2016). Flood hazard and risk assessment using GIS and remote sensing in lower Awash sub-basin, Ethiopia. *Journal of Environment and Earth Science*, 6(9), 69–86.
- Wu, T., Li, J., Li, T., Sivakumar, B., Zhang, G., & Wang, G. (2019). High-efficient extraction of drainage networks from digital elevation models constrained by enhanced flow enforcement from known river maps. *Geomorphology*, 340, 184–201. <https://doi.org/10.1016/j.geomorph.2019.04.022>.
- Zeleňáková, M., Fijko, R., Labant, S., Weiss, E., Markovič, G., & Weiss, R. (2019). Flood risk modelling of the Slatvinec stream in Kružlov village, Slovakia. *Journal of Cleaner Production*, 212, 109–118. <https://doi.org/10.1016/j.jclepro.2018.12.008>.
- Zheng, X., Maidment, D. R., Tarboton, D. G., & ... (2018). GeoFlood: Large-scale flood inundation mapping based on high-resolution terrain analysis. *Water Resources ...* <https://doi.org/10.1029/2018WR023457>. <https://doi.org/10.1029/2018WR023457>.